

Supplement to “Analysis of reactive bromine production and ozone depletion in the Arctic boundary layer using 3-D simulations with GEM-AQ: Inference from synoptic-scale patterns”

K. Toyota^{1,2}, J. C. McConnell¹, A. Lupu¹, L. Neary^{1,†}, C. A. McLinden², A. Richter³, R. Kwok⁴, K. Semeniuk¹, J. W. Kaminski¹, S.-L. Gong², J. Jarosz¹, M. P. Chipperfield⁵, and C. E. Sioris²

¹Department of Earth and Space Science and Engineering, York University, Toronto, Ontario, Canada

²Air Quality Research Division, Science and Technology Branch, Environment Canada, Toronto, Ontario, Canada

³Institute of Environmental Physics, University of Bremen, Bremen, Germany

⁴Jet Propulsion Laboratory, California Institute of Technology, Pasadena, California, USA

⁵School of Earth and Environment, University of Leeds, Leeds, UK

[†]Now at Belgian Institute for Space Aeronomy (BIRA-IASB), Brussels, Belgium

April 20, 2011

S1 Surface winds and temperatures simulated by GEM

Simulated surface winds and temperatures are evaluated by using routine and research observational data obtained at the ground level across the Arctic (red stars in Fig. 2 of the main paper). Table S1 presents statistical metrics from the comparison between the simulation and the observations at each site. We used observational data available electronically from several sources: National Climatic Data Center (NCDC, <http://www.ncdc.noaa.gov/>) for routine observations maintained by various national bureaus; NOAA/ESRL Global Monitoring Division (<http://www.esrl.noaa.gov/gmd/>) for data from Barrow, Alaska; Norwegian Institute for Air Research (<http://www.nilu.no/niluweb/services/zeppelin/>) for data from Zeppelin, Svalbard, Norway; Environment Canada (<http://www.msc-smc.ec.gc.ca/natchem/>) for data from the Alert GAW station, Ellesmere Island, Canada (Environment Canada, 2001); and National Snow and Ice Data Center (<http://nsidc.org/>) for data from the J-CAD 3 buoy drifting near the North Pole during our simulation period (Kikuchi et al., 2004; Inoue and Kikuchi, 2007). Nominally all of these meteorological data are hourly archives. However, for more than half of the NCDC data used here, the actual time resolution of archived data is 6 hour.

In general, temporal variations in the surface wind speeds and directions are simulated reasonably well at sites located within smooth topography, such as Barrow, Resolute, Inuvik, Ostrov Kotelnij, Ostrov Golomjannyj and the J-CAD 3 buoy (see Figs. S1c–d,f and correlation coefficients between the simulations and observations in Table S1). This suggests that the boundary-layer meteorology at these sites was largely under the control of synoptic- and/or planetary-

scale forcing resolved well at the grid resolution used in the present simulation. For example, Fig. 9a of the main paper shows surface air temperatures and wind vectors simulated at 12 UTC for each day between 15–22 April 2001. During this period, major disturbances in the Arctic surface meteorology had spatial scales of apparently greater than 1000 km, while their emergence, migration and disappearance could be tracked well at daily interval. Strong surface winds, accompanied quite often by increased surface air temperatures, were associated with a bipolar development of the high and low pressure systems evident in the 850 hPa height fields (Fig. S2a). The 500 hPa height fields developed the same horizontal structures largely in phase with the 850 hPa height fields (Fig. S2b), indicating a formation of blocking highs and lows as the major cause of large-scale disturbances during this period (Pelly and Hoskins, 2003; Croci-Maspoli et al., 2007; Tyrlis and Hoskins, 2008a,b).

Polar lows also create major disturbances to the surface meteorology in the Arctic. They are intense mesocyclones that form over the Arctic and sub-arctic open ocean where colder air masses advected from adjacent terrestrial regions or from over the frozen ocean create a strong thermal instability in the lower atmosphere (Rasmussen and Turner, 2003). However, the climatology of their migration to the ice-covered ocean in the Arctic is poorly characterized, because ground observations are scarce and the identification of clouds from conventional meteorological satellites is quite difficult over the sea ice (e.g., Serreze and Barry, 1988; Blechschmidt, 2008). Given their short-lived nature and relatively small spatial scales, we do not expect that the present model simulation has captured a majority of the polar lows that actually occurred during the simulated period. Nevertheless, the model apparently did a reasonable job in simulating one outstanding episode during 6–7 April 2001 when a in-

Correspondence to: K. Toyota (kenjiro.toyota@ec.gc.ca)

Table S1. Statistical metrics from a comparison between observed and simulated hourly surface air temperatures and winds at selected Arctic sites^a during April 2001: Vector correlation coefficients between observed and simulated surface winds (r_V)^b, scalar correlation coefficients between observed and simulated surface wind speeds (r_S), number of samples (n), monthly means and standard deviations for observed surface wind speeds (S_{obs}), mean biases (B_S) and root mean squared errors (E_S) for simulated surface wind speeds, correlation coefficients between observed and simulated surface air temperatures (r_T), monthly means and standard deviations for observed surface air temperatures (T_{obs}), and mean biases (B_T) and root mean squared errors (E_T) for simulated surface air temperatures.

	Wind statistics						Temperature statistics				
	r_V	r_S	n	S_{obs} [m/s]	B_S [m/s]	E_S [m/s]	r_T	n	T_{obs} [°C]	B_T [°C]	E_T [°C]
Alert CFS	0.58	0.44	174	3.1±3.3	+0.0	2.9	0.85	238	-25.6 ± 5.9	-0.5	3.2
Alert GAW	0.74	0.57	719	3.2±3.8	-0.3	3.2	0.86	720	-23.7 ± 6.4	-2.4	4.1
Barrow	1.20	0.83	646	5.6±3.1	+0.5	2.1	0.87	665	-16.9 ± 4.7	-1.3	2.9
Eureka	0.57	0.32	466	3.2±3.2	-0.1	3.0	0.90	651	-25.3 ± 7.0	+0.5	3.1
Hall Land	0.80	0.44	194	4.2±2.9	+1.0	3.2	n.a.	0	n.a.	n.a.	n.a.
Inuvik	0.92	0.50	674	3.1±1.5	+0.2	1.6	0.85	714	-11.2 ± 6.5	-3.2	4.7
Resolute	0.89	0.70	610	5.6±3.9	-1.3	3.1	0.80	705	-22.2 ± 4.7	-2.5	4.5
Golomjannyj	0.95	0.64	231	5.4±3.0	-0.9	2.5	0.79	232	-23.9 ± 4.4	-3.5	4.8
Kotelnyj	1.07	0.76	225	6.9±4.1	-1.3	3.1	0.92	232	-20.4 ± 5.3	-1.2	2.6
Vrangeljja	0.92	0.43	150	4.4±3.6	+0.4	3.4	0.86	187	-15.7 ± 4.8	-3.0	3.9
Ny Ålesund	0.29	0.50	230	2.9±2.6	+2.2	3.6	0.94	234	-11.0 ± 7.1	+1.4	3.0
Zeppelin	0.66	0.50	650	2.7±1.9	+4.0	5.2	0.96	720	-12.4 ± 6.7	+0.1	1.9
J-CAD 3 buoy	0.97	0.65	447	3.0±1.5	+1.8	2.6	0.85	505	-21.8 ± 5.7	-2.3	5.0

Note: ^aThe location of each station is indicated in Fig. 2a–b of the main paper; ^bCalculated following Crosby et al. (1993), $-\sqrt{2}$ for the perfect anti-correlation and $\sqrt{2}$ for the perfect correlation.

tense, closed vortex migrated from the south through Bering Strait (Fig. S3a–b). While the vortex had weakened by the time it approached Barrow on 8 April, the warm advection from the south associated with this system led to an increase in the surface air temperature as large as 10 K at Barrow on 7 April (Fig. S1c).

On the other hand, the model does not perform as well at the present grid resolution for simulating the surface winds near or within mountains, such as at Alert CFS/GAW, Eureka, Ny Ålesund, and Zeppelin (Table S1 and Fig. S1a,e). For example, downslope flows are induced by a surface radiative cooling and are known to prevail in the shallow layer of the lowest atmosphere over Greenland (e.g., Bromwich et al., 1996; Cassano et al., 2001) and also around Alert in the northeastern slope of Ellesmere Island (e.g., Hopper et al., 1998; Persson and Stone, 2007). The grid resolution of our model appears to be too coarse properly to resolve the topography which creates downslope flows at Alert (Persson and Stone, 2007, see Fig. 8). Note, however, that temporal variations in surface air temperature and wind speed/direction at Hall Land, Greenland, located across the channel from Alert (see Fig. 2b of the main paper) show some coherence with those observed at Alert (Fig. S1a–b). In addition, the coherent part of the temperature/wind variations observed at two Alert stations and Hall Land appears to be captured reasonably well by the model. Thus, while the boundary-layer meteorology at Alert is influenced strongly by unresolved meso-scale flows, the model apparently did a reasonable job in simulating synoptic disturbances (except secondary meso-scale

flows) around the site.

There were five prominent cases of short-lived wind episodes observed at the Alert GAW station on 9, 11, 24, 25 and 28 April, which appeared to be associated with the downslope flow. However, none of these episodes is captured reasonably enough by our model. During these episodes, the wind speed at Alert GAW abruptly increased to 10–15 m s⁻¹ and lasted only for several hours. The wind direction was southerly to southwesterly, typical of the downslope flow at Alert (Persson and Stone, 2007). Except for the case on 28 April when the surface wind speed concurrently increased at Alert CFS, those windy episodes were not observed at Alert CFS or Hall Land, indicating the limited horizontal and vertical scales of the phenomena. The surface air temperature also increased by as high as 10 K during the events, indicating that these air masses had been transported from and/or mixed with air masses in the free troposphere. This also explains the concurrent increase in the surface ozone mixing ratios observed at the Alert GAW station (Fig. 3a of the main paper). Foehn storms characterized by strong southwesterly winds have been observed during the wintertime at Alert with a concurrent increase in temperature sometimes by more than 20 K in a few hours (Maxwell, 1980).

On many occasions, simulated wind speeds at two stations in Svalbard, Norway, viz. Ny Ålesund and Zeppelin, are too high as compared to the observations (Table S1 and Fig. S1e). The unresolved topography appears to be one of the reasons for this failure. Also, since these sites are located near the boundary between the open and frozen oceans, spatial varia-

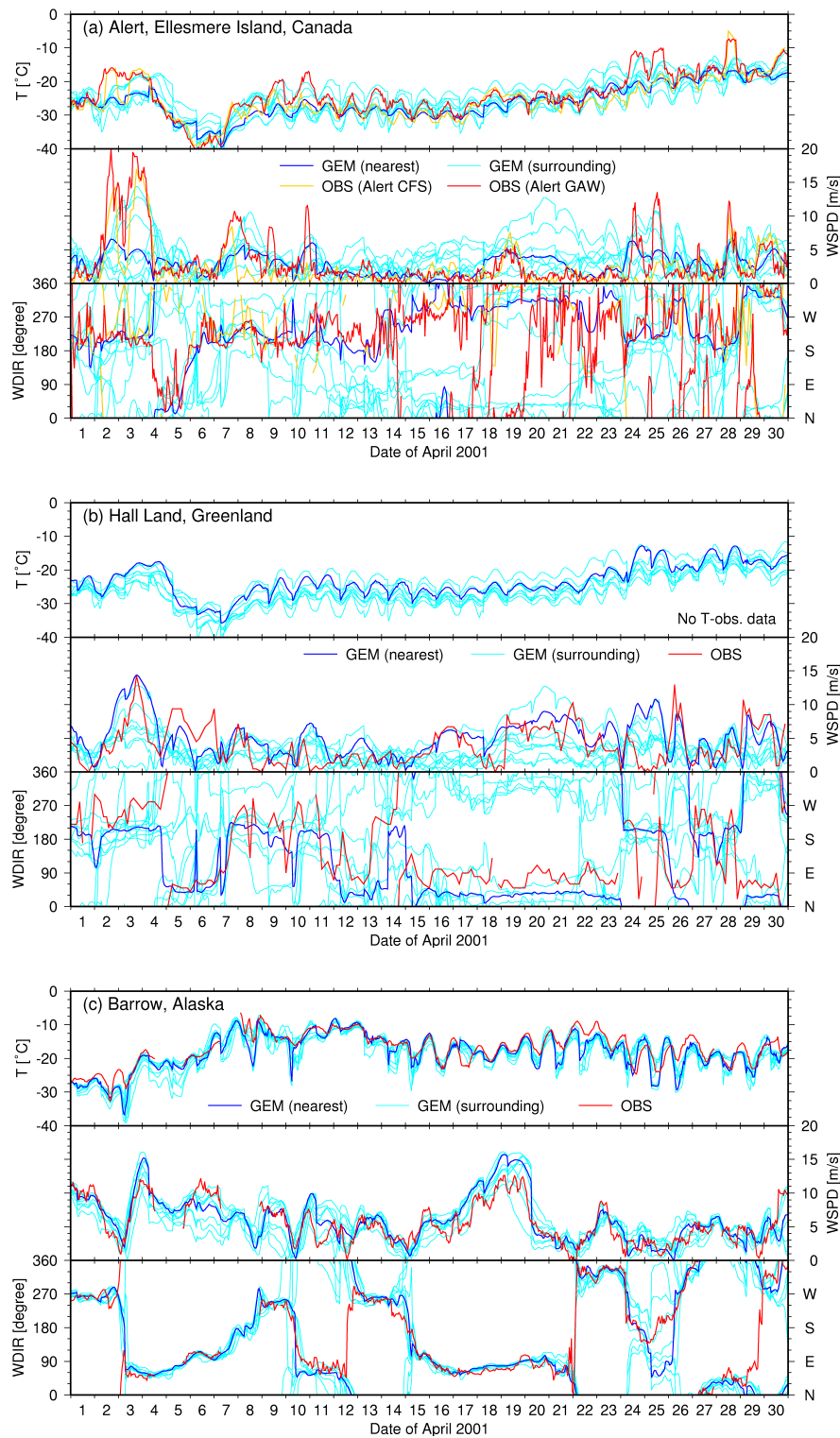


Fig. S1. Hourly surface air temperatures and wind speeds/directions observed at (a) Alert CFS (orange lines) and GAW (red lines) stations, Ellesmere Island, Canada, (b) Hall Land, Greenland, (c) Barrow NOAA/ESRL station, Alaska, (d) Ostrov Golomjannyj, Russia, (e) Zeppelin, Svalbard, Norway, and (f) the JAMSTEC Compact Arctic Drifter (J-CAD) 3 buoy drifting near the north pole, plotted along with corresponding variables simulated by the GEM model at the nearest (blue lines) and 8 surrounding (light blue lines) grid cells. The simulated values are taken from the lowest model level, except for Zeppelin where the 4th lowest vertical model level (~ 470 m a.s.l.) is chosen to best match the altitude of the station.

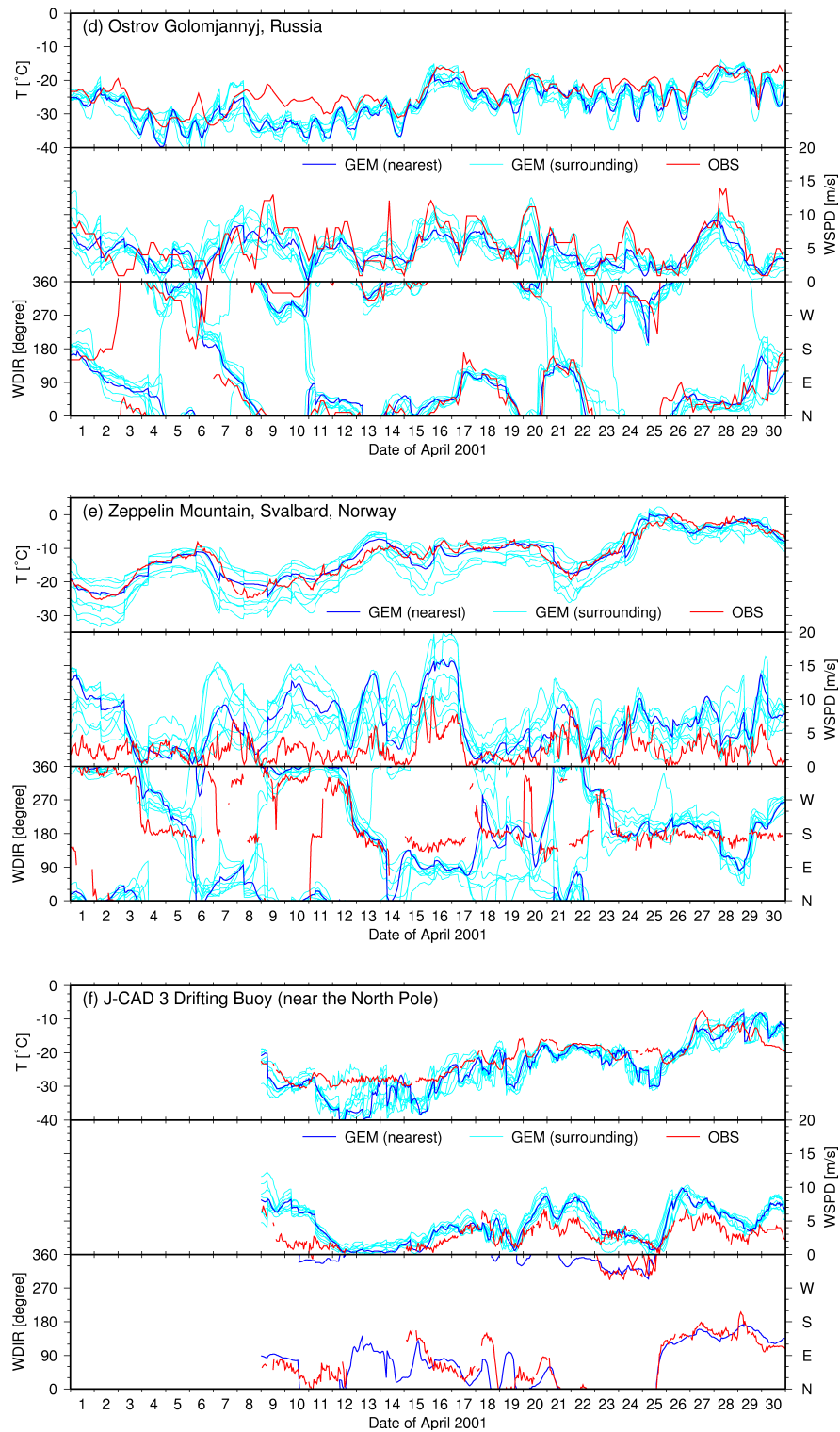


Fig. S1. (Continued.)

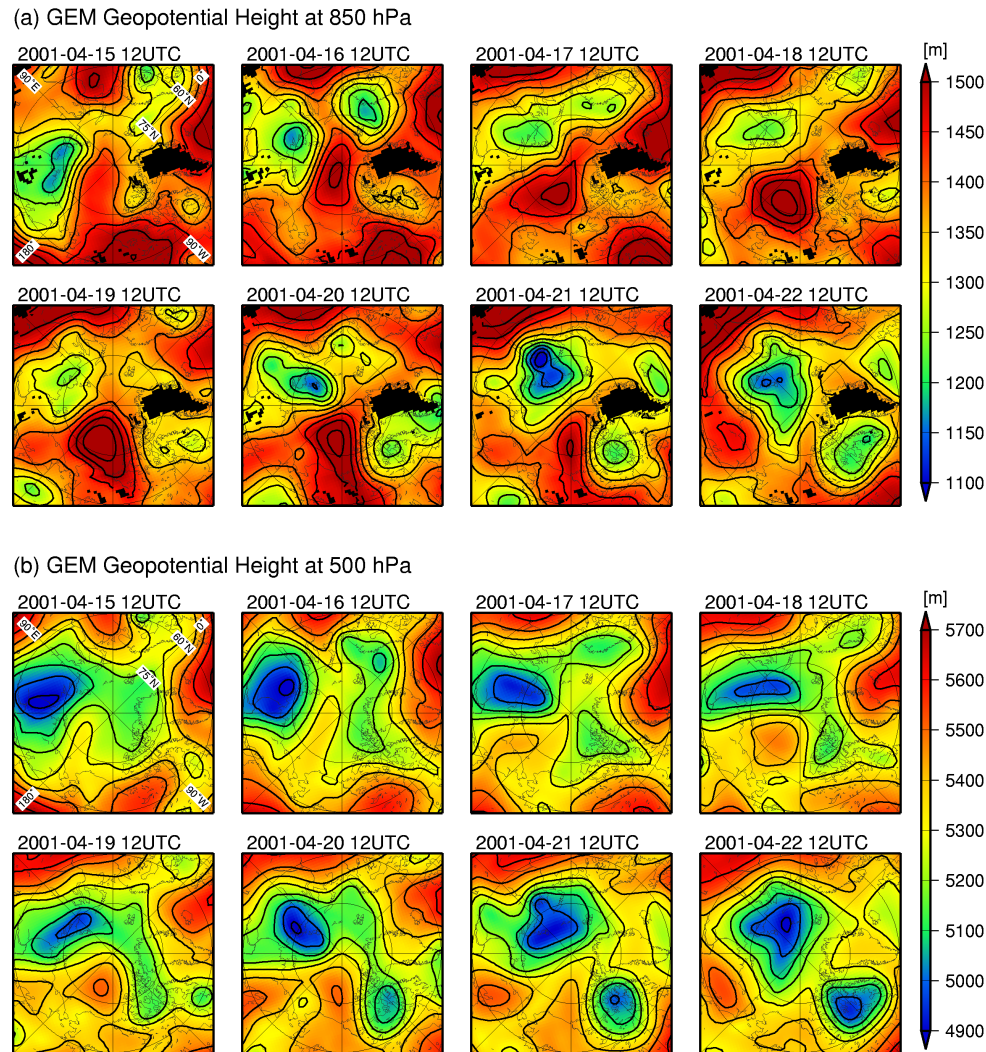


Fig. S2. (a) Geopotential height fields (contoured every 50 m) at 850 hPa level at 12 UTC for each day between 15–22 April 2001 simulated by the GEM model; and (b) The same as (a) but for geopotential height (contoured every 100 m) at 500 hPa level.

tions in the heat supply to the atmosphere (as a driving force of polar lows and other meso-scale circulations) may not have been resolved very well at the present grid resolution.

Correlation coefficients between the simulated and observed surface air temperatures are generally higher than 0.8 (Table S1). While diurnal variations in the temperature play a role here, the variability at timescales of longer than 1 day is also simulated reasonably well at many sites (Fig. S1a-f). This indicates again the good capability of the model in simulating the synoptic disturbances.

However, for most of the sites examined here, simulated surface air temperatures exhibit a cold bias of -0.5 K to -3.5 K in the monthly mean against the observations (Table S1). It is possible that the quality of the observational data is rather questionable, because automated meteorological observations are quite challenging in the cold, high-latitude en-

vironment owing to possible physical interferences to the instruments such as a formation of frost and snowdrift. We note, however, some consistency for the occurrence of the cold bias in simulated surface air temperatures. It appears that the model simulates an excessive radiative cooling at the surface and in the near-surface air during the night under the calm atmosphere (Fig. S1c–d and f). Fortunately, as discussed in Sect. 3 of the main paper, bromine release from the snowpack is simulated to occur most actively when/where the surface wind speed is high. Therefore the issue of the cold bias would not undermine our discussion too much when it comes to the impacts of temperature on the bromine release.

In the polar lower troposphere, when the air is cooled rapidly under the clear sky, a “diamond dust” will be formed via condensation of water vapor. This process can signif-

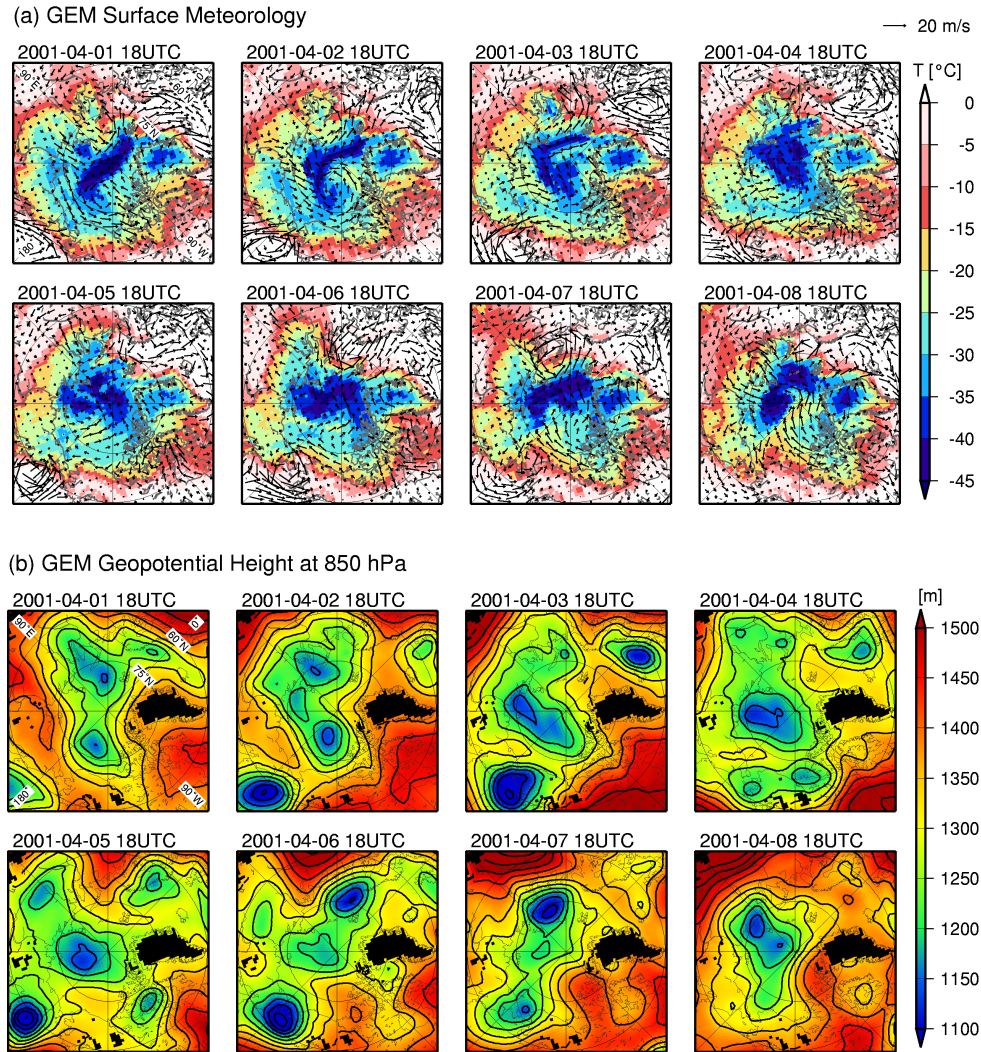


Fig. S3. (a) Surface air temperatures (color shade, in C) and wind vectors (arrow length for the wind speed of 20 m s^{-1} is indicated in the top right corner) at 18 UTC for each day between 1–8 April 2001 simulated by the GEM model; and (b) The same as (a) but for geopotential height fields (contoured every 50 m) at 850 hPa level.

icantly slow down the surface radiative cooling from what would otherwise occur at the rate of sometimes more than 20 K day^{-1} in the clear sky (Curry, 1983; Curry and Ebert, 1992; Walsh and Chapman, 1998). It is a very intricate process and requires a parameterization for cloud microphysics dedicated to simulating the diamond dust, which, to our knowledge, has not been implemented to operational weather forecast models. Also, the reliability of radiative transfer calculations for the polar atmosphere often becomes questionable in the presence of clouds, because parameterizations for the cloud and precipitation processes are, in general, simply “re-used” from what have been validated for simulations outside the polar region (e.g., Inoue et al., 2006).

It should be noted that the present meteorological simulation does not necessarily comply with the most recent ver-

sion of GEM in use for operational weather forecasts. Also, in a model inter-comparison study by Cuxart et al. (2006), the turbulent-diffusivity parameterization used in GEM was found to perform among the best of the operational/research models tested for the simulation of scalar profiles in a stably stratified boundary layer typical of the Arctic. The simulated meteorology examined here could have been in better agreement with the observations by choosing a more sophisticated package for cloud physics and/or by running the model at higher resolutions (e.g., Mailhot et al., 2002). The configuration and grid resolution of the present model are chosen so as to perform many model runs within a reasonable computational time for adjusting empirical parameters related to the air-snowpack chemical interactions.

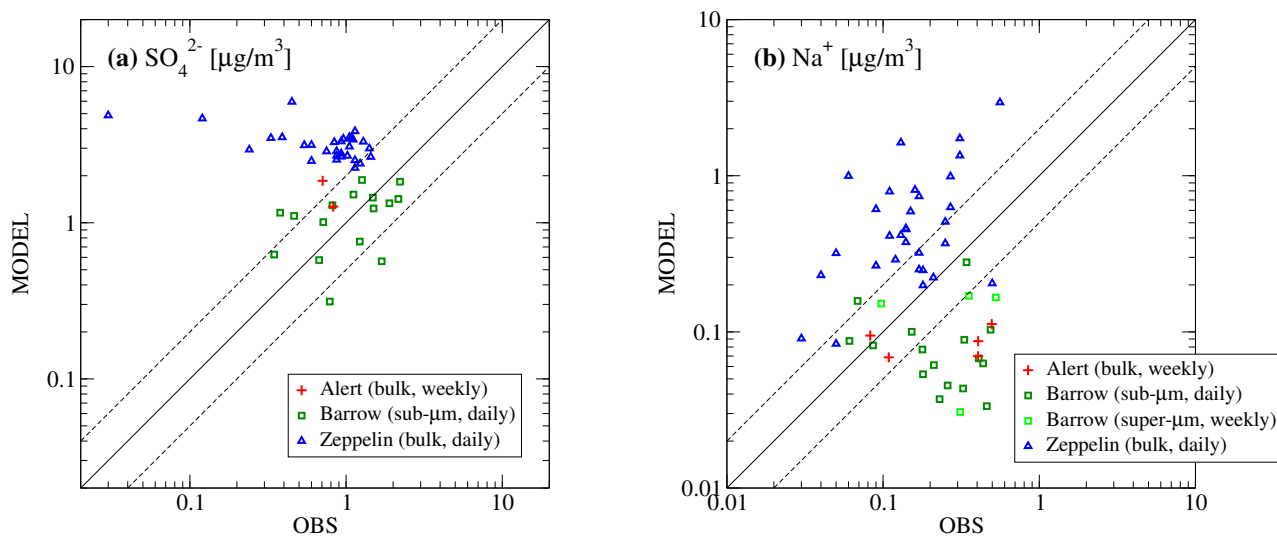


Fig. S4. Scatter plots of simulated non-sea-salt sulfate (a) and sodium (b) concentrations (from Run 3) versus observations at the ground level from three Arctic stations during April 2001 (Quinn et al., 2007): Alert, Canada (electronic data are available from the Canadian National Atmospheric Chemistry Database at <http://www.msc.ec.gc.ca/natchem/>); Barrow, Alaska (electronic data are available from the Pacific Marine Environmental Laboratory, National Oceanic and Atmospheric Administration at <http://saga.pmel.noaa.gov/data/>); and Zeppelin, Svalbard (electronic data are available from the European Monitoring and Evaluation Programme at <http://www.emep.int/>). In each graph, data points bounded between broken lines indicate agreement within a factor of two. The observational data were obtained by analyzing either bulk or size-resolved (submicron and supermicron) aerosol samples collected on the daily to weekly basis. The size-segregated sulfate and sea-salt aerosol concentrations simulated by the model are averaged in time and integrated over size bins so as to match sampling intervals and methods employed for the corresponding field data. The mass ratio of sodium to dry sea salt is assumed to be 30.77% (Gong et al., 2003).

S2 Ground-level aerosol concentrations simulated by GEM-AQ

While it is beyond the scope of the present study to evaluate simulated aerosol concentrations in detail, we briefly compared the simulated sulfate and sea-salt aerosol concentrations with the observations (as non-sea-salt sulfate and sodium, respectively) at the ground level from three Arctic sites (Fig. S4).

For the non-sea-salt sulfate, agreement between the simulation and the observations is generally within a factor two except at Zeppelin, Svalbard where the model simulates 3 to 5 times greater concentrations in a majority of cases. For the sodium, more than half of the cases are outside the range of agreement within a factor of two, either by overprediction or by underprediction, at the three sites examined here. This is not surprising, partly because our model does not include the production mechanisms of sea-salt aerosols via frost flowers abrasion (Rankin et al., 2002) and via blowing snow sublimation (Yang et al., 2008). At Zeppelin, the overprediction of the sea-salt aerosol concentrations is most likely caused by an issue with the source term around the site arising from the bias in the simulated surface wind speed (see Sect. S1). Fortunately, the simulated and observed concentrations of sea-salt aerosols are both smaller than those of sulfate aerosols mostly by more than an order of magnitude. Therefore, the

sulfate aerosols, which are simulated better and reasonably well, play a major role in controlling the rates of heterogeneous reactions of inorganic bromine species (Reactions G130–132) in our model runs.

As discussed in Sect. 3.1 of the main paper, the overprediction of the sulfate aerosol concentrations at Zeppelin may be partially responsible for unrealistically strong bromine activation simulated around this site. Nevertheless, considering challenges faced by state-of-the-art aerosol transport models in simulating physical processes such as a precipitation scavenging and a long-range transport occurring in the Arctic (Korhonen et al., 2008; Shindell et al., 2008), the general capability of our model is quite satisfactory.

S3 Back-trajectories from Alert, Barrow and Zeppelin

In an attempt to gain an insight into a possible link between “BrO clouds” and subsequent ODEs at downwind locations in our simulations, we looked at trajectories of air parcels going back from three Arctic locations that correspond to Alert, Barrow and Zeppelin.

Fig. S5 shows the 5-day backward trajectories from Alert, Barrow and Zeppelin at three pressure levels (950, 900 and 850 hPa) for each day between 15–22 April 2001, generated by the Canadian Meteorological Centre (CMC) trajec-

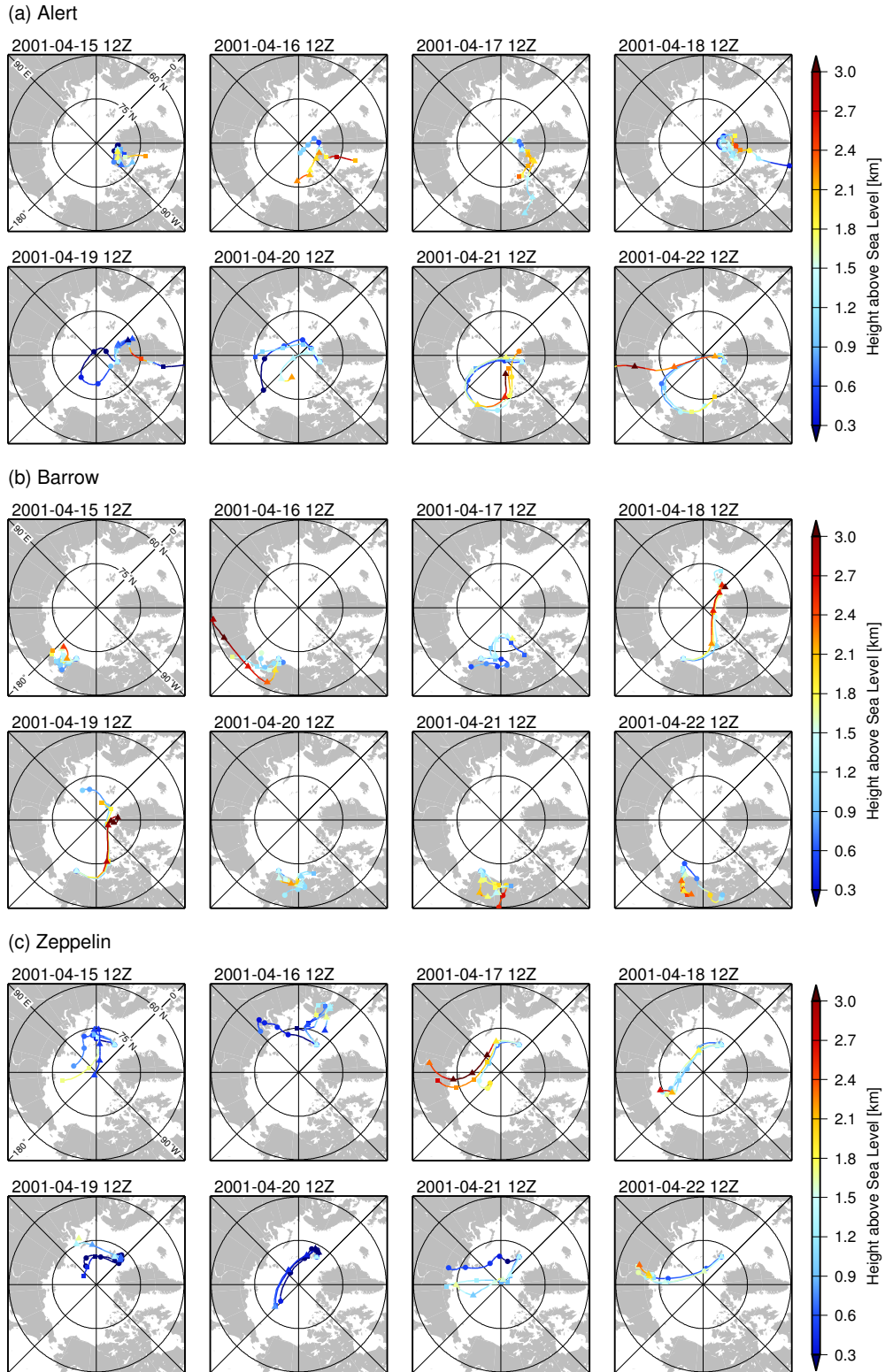


Fig. S5. (a) 5-day backward trajectories going back from Alert at 950, 900 and 850 hPa levels (marked by circles, squares and triangles, respectively, indicating the location of air parcels at 24-hour intervals) at 12 UTC for each day between 15–22 April 2001. The height of air parcels above the sea level is also indicated by the color shade; (b) The same as (a) but backward trajectories from Barrow; and (c) The same as (a) but backward trajectories from Zeppelin.

tory model (Stocki et al., 2005; Sharma et al., 2006; Chan and Vet, 2010). The model uses 3-D wind fields generated by the operational GEM model during the process of weather forecasts at CMC (D'Amours, R. and Pagé, P., Atmospheric transport models for environmental emergencies, CMC internal document, Canadian Meteorological Centre, Dorval, Quebec, 2001). The model resolution and the physical parameterizations employed for CMC's weather forecasts are somewhat different from those employed for GEM-AQ simulations in this study. Therefore the trajectories obtained are not necessarily consistent with the advection in our model runs and should be viewed with some caution.

Some interpretations from these trajectories are presented in Sect. 3.2 of the main paper.

References

- Blechschmidt, A.-M.: A 2-year climatology of polar low events over the Nordic Seas from satellite remote sensing, *Geophys. Res. Lett.*, 35, L09 815, doi:10.1029/2008GL033706, 2008.
- Bromwich, D. H., Du, Y., and Hines, K. M.: Wintertime surface winds over the Greenland ice sheet, *Mon. Wea. Rev.*, 124, 1941–1947, 1996.
- Cassano, J. J., Box, J. E., Bromwich, D. H., Li, L., and Steffen, K.: Evaluation of Polar MM5 simulations of Greenland's atmospheric circulation, *J. Geophys. Res.*, 106, 33 867–33 889, 2001.
- Chan, E. and Vet, R. J.: Baseline levels and trends of ground level ozone in Canada and the United States, *Atmos. Chem. Phys.*, 10, 8629–8647, 2010.
- Croci-Maspoli, M., Schwierz, C., and Davies, H. C.: A multifaceted climatology of atmospheric blocking and its recent linear trend, *J. Climate*, 20, 633–649, 2007.
- Crosby, D. S., L. C. Breaker, L. C., and Gemmill, W. H.: A proposed definition for vector correlation in geophysics: Theory and application, *J. Atmos. Oceanic Technol.*, 10, 355–367, 1993.
- Curry, J.: On the formation of continental polar air, *J. Atmos. Sci.*, 40, 2278–2292, 1983.
- Curry, J. A. and Ebert, E. E.: Annual Cycle of Radiation Fluxes over the Arctic Ocean: Sensitivity to Cloud Optical Properties, *J. Climate*, 5, 1267–1280, 1992.
- Cuxart, J., Holtzlag, A. A. M., Beare, R. J., Bazile, E., Beljaars, A., Cheng, A., Conangla, L., Ek, M., Freedman, F., Hamdi, R., Kerstein, A., Kitagawa, H., Lenderink, G., Lewellen, D., Mailhot, J., Mauritsen, T., Perov, V., Schayes, G., Steeneveld, G.-J., Svensson, G., Taylor, P., Weng, W., Wunsch, S., and Xu, K.-M.: Single-column model intercomparison for a stably stratified atmospheric boundary layer, *Boundary-Layer Meteorol.*, 118, 273–303, 2006.
- Environment Canada: Canadian National Atmospheric Chemistry (NAChem) Database, 2001.
- Gong, S. L., Barrie, L. A., Blanchet, J. P., von Salzen, K., Lohmann, U., Lesins, G., Spacek, L., Zhang, L. M., Girard, E., Lin, H., Leaitch, R., Leighton, H., Chylek, P., and Huang, P.: Canadian Aerosol Module: A size-segregated simulation of atmospheric aerosol processes for climate and air quality models 1. Module development, *J. Geophys. Res.*, 108(D1), 4007, doi:10.1029/2001JD002002, 2003.
- Hopper, J. F., Barrie, L. A., Silis, A., Hart, W., Gallant, A. J., and Dryfhout, H.: Ozone and meteorology during the 1994 Polar Sunrise Experiment, *J. Geophys. Res.*, 103, 1481–1492, 1998.
- Inoue, J. and Kikuchi, T.: Outflow of summertime Arctic sea ice observed by ice drifting buoys and its linkage with ice reduction and atmospheric circulation patterns, *J. Meteorol. Soc. Japan*, 85, 881–887, 2007.
- Inoue, J., Liu, J., Pinto, J. O., and Curry, J. A.: Intercomparison of Arctic regional climate models: Modeling clouds and radiation for SHEBA in May 1998, *J. Climate*, 19, 4167–4178, 2006.
- Kikuchi, T., Hatakeyama, K., and Morison, J. H.: Distribution of convective lower halocline water in the eastern Arctic Ocean, *J. Geophys. Res.*, 109, C12 030, doi:10.1029/2003JC002223, 2004.
- Korhonen, H., Carslaw, K. S., Spracklen, D. V., Ridley, D. A., and Ström, J.: A global model study of processes controlling aerosol size distributions in the Arctic spring and summer, *J. Geophys. Res.*, 113, D08 211, doi:10.1029/2007JD009114, 2008.
- Mailhot, J., Tremblay, A., Bélair, S., Gultepe, I., and Isaac, G. A.: Mesoscale simulation of surface fluxes and boundary layer clouds associated with a Beaufort Sea polynya, *J. Geophys. Res.*, 107(C10), 8031, doi:10.1029/2000JC000429, 2002.
- Maxwell, J. B.: The Climate of the Canadian Arctic Islands and Adjacent Waters, vol. 1, Climatological Series No. 30, Environment Canada, Atmospheric Environment Service, 1980.
- Pelly, J. L. and Hoskins, B. J.: A new perspective on blocking, *J. Atmos. Sci.*, 60, 743–755, 2003.
- Persson, P. O. G. and Stone, R.: Evidence of forcing Arctic regional climates by mesoscale processes, in: AMS Symposium on Connections between Mesoscale Processes and Climate Variability, 15–16 January 2007, San Antonio, TX, American Meteorological Society, URL http://ams.confex.com/ams/87ANNUAL/techprogram/paper_119015.htm, 2007.
- Quinn, P. K., Shaw, G., Andrews, E., Dutton, E. G., Ruoho-Airola, T., and Gong, S. L.: Arctic haze: current trends and knowledge gaps, *Tellus*, 59B, 99–114, 2007.
- Rankin, A. M., Wolff, E. W., and Martin, S.: Frost flowers: Implications for tropospheric chemistry and ice core interpretation, *J. Geophys. Res.*, 107(D23), 4683, doi:10.1029/2002JD002492, 2002.
- Rasmussen, E. A. and Turner, J.: Polar Lows: Mesoscale Weather Systems in the Polar Regions, Cambridge Univ. Press, Cambridge, UK, 2003.
- Serreze, M. C. and Barry, R. G.: Synoptic activity in the Arctic basin, 1979–85, *J. Climate*, 1, 1276–1295, 1988.
- Sharma, S., Andrews, E., Barrie, L. A., Ogren, J. A., and Lavoué, D.: Variations and sources of the equivalent black carbon in the high Arctic revealed by long-term observations at Alert and Barrow: 1989–2003, *J. Geophys. Res.*, 111, D14 208, doi:10.1029/2005JD006581, 2006.
- Shindell, D. T., Chin, M., Dentener, F., Doherty, R. M., Faluvegi, G., Fiore, A. M., Hess, P., Koch, D. M., MacKenzie, I. A., Sanderson, M. G., Schultz, M. G., Schulz, M., Stevenson, D. S., Teich, H., Textor, C., Wild, O., Bergmann, D. J., Bey, I., Bian, H., Cuvelier, C., Duncan, B. N., Folberth, G., Horowitz, L. W., Jonson, J., Kaminski, J. W., Marmer, E., Park, R., Pringle, K. J., Schroeder, S., Szopa, S., Takemura, T., Zeng, G., Keating, T. J., and Zuber, A.: A multi-model assessment of pollution transport to the Arctic, *Atmos. Chem. Phys.*, 8, 5353–5372, 2008.

- Stocki, T., Blanchard, X., D'Amours, R., Ungar, R., Fontaine, J., Sohler, M., Bean, M., Taffary, T., Racine, J., Tracy, B., Brachet, G., Jean, M., and Meyerhof, D.: Automated radioxenon monitoring for the comprehensive nuclear-test-ban treaty in two distinctive locations: Ottawa and Tahiti, *J. Environ. Radioactivity*, 80, 305–326, 2005.
- Tyrlis, E. and Hoskins, B. J.: Aspects of a Northern Hemisphere atmospheric blocking climatology, *J. Atmos. Sci.*, 65, 1638–1652, 2008a.
- Tyrlis, E. and Hoskins, B. J.: The morphology of Northern Hemisphere blocking, *J. Atmos. Sci.*, 65, 1653–1665, 2008b.
- Walsh, J. E. and Chapman, W. L.: Arctic Cloud–Radiation–Temperature Associations in Observational Data and Atmospheric Reanalyses, *J. Climate*, 11, 3030–3045, 1998.
- Yang, X., Pyle, J. A., and Cox, R. A.: Sea salt aerosol production and bromine release: Role of snow on sea ice, *Geophys. Res. Lett.*, 35, L16 815, doi:10.1029/2008GL034536, 2008.